Measuring muon neutrino disappearance with the NOvA experiment

Luke Vinton

Declaration

I hereby declare that this thesis has not been and will not be submitted in whole or in part to another University for the award of any other degree.

Signature:

Luke Vinton

UNIVERSITY OF SUSSEX

Luke Vinton, Doctor of Philosophy

Measuring muon neutrino disappearance with the NOvA experiment

Summary

Abstract

Acknowledgements

Contents

List of Tables

List of Figures

Chapter 1

Introduction

Chapter 2

Neutrino Physics

2.1 The Standard Model

Our current understanding of particle physics is well described by the Standard model, which describes the interactions between fundamental particles and the weak, electromagnetic and strong forces.

2.2 The Weak Force

Neutrinos interact with matter through the weak force in one of three flavour eigenstates (electron, muon or tau). The weak force is mediated by the electrically charged $W^{\pm}$ and electrically neutral Z bosons.

Include feynam diagrams of the neutrino interactions.

A neutrino interacting with matter through the W boson will produce a charged lepton corresponding to the weak flavour of the incoming neutrino. This process can happen in reverse, with a charged lepton producing a neutrino with the same flavour and a W boson. Such processes involving a W boson are known as charged current interactions (CC interactions).

2.3 Neutrino Oscillations

As current understanding has it, neutrinos come in three eigenstates of the weak force (electron, muon and tau) and three mass eigenstates (m_1, m_2 or m_3). The weak eigenstates do not correspond directly to the mass eigenstates. Instead, the weak eigenstates are a superposition of the mass states and vice versa.

Once produced, neutrinos propogate as a superposition of mass eigenstates

2.4 Need to include the following

Meson decay for neutrino beam production

Chapter 3

The NOvA Experiment

The NOvA experiment (NuMI Off-axis ν_e Appearance) consists of two detectors which measure the neutrino composition of the NuMI (Neutrinos at the Main Injector) beam. The 300 ton near detector is located on site at Fermilab 1.015 km from the NuMI target. The 14 kiloton far detector is located at a site near Ash River Minnesota and is 810km from the NuMI target. Both detectors are placed off-axis from the centre of the NuMI beam by 14.6 mrads.

The original design of the NOvA experiment is laid out in the technical design report (TDR) [1]. The constructed experiment differs only slightly with the design laid out in the TDR. The details of the constructed experiment, including the neutrino beam source and the two detectors, are discussed in the following chapter.

3.1 The NuMI Beam

The NOvA experiment's neutrino source is provided by the Neutrinos at the Main Injector (NuMI) beam at Fermilab. The following section describes the process by which the NuMI muon neutrino beam is created.

An instructive diagram of the NuMI beam facility is presented in Figure 3.1. The Main Injector accepts six batches, each spanning 10 μsec, of protons at a time and accelerates the protons up to 120 GeV. A 10 μs pulse of accelerated protons, known as a beam spill, is directed to collide with the 95 cm long graphite target every 1.33 s.

The collision of the accelerated protons with the carbon atoms of the target produce a plethora of secondary particles (mostly pions and kaons). The charged mesons are focused into a beam by two magnetic focussing horns. The focussed beam of charged mesons then travels through a 675 m long evacuated decay pipe. Along this length of pipe the mesons

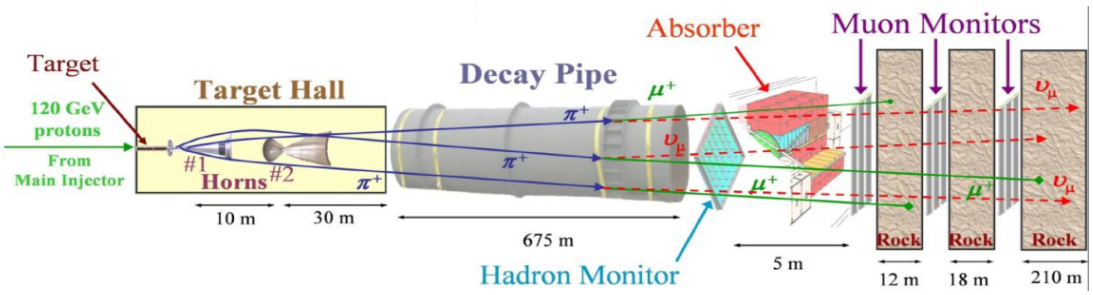

Figure 3.1: A diagram showing the layout of the NuMI beam.

decay predominantly to charged leptons and neutrinos. The decay pipe is followed by hadron and muon monitors and about 240m of rock. The rock absorbs the remaining charged particles in the beam before reaching the near detector.

Details of the focussing horns and off-axis detector detector position are provided in the following subsections.

3.1.1 Focussing Horns

Focussing horns are used to focus the mesons, created by collisions of protons with the NuMI target, into a beam. Changing the current direction within the magnetic focussing horns changes the sign of the mesons that are focussed. The focussing horns are run in Forward Horn Current (FHC) or Reverse Horn Current (RHC) mode to select positively or negatively charged mesons respectively, leading to a neutrino or an anti-neutrino beam respectively.

3.1.2 Off-axis Detectors

The NOvA detectors are both placed 14 mrads off the axis of the NuMI beam. The reasons for placing the detector will be described in more detail in the following paragraphs.

The decay used to produce a neutrino beam is a two body decay, where a pion (or kaon) decays to a neutrino and a muon. The two body decay occurs isotropically in the parent particles rest frame. In the lab frame the parent particle is not at rest when decaying. For pion and kaon decay this boosts the neutrinos into a cone in the direction of the parent particle. For small angles, the flux and energy of neutrinos produced by pion decay ($\pi \rightarrow \nu_\mu + \mu$) are given by:

$$\Phi = \left(\frac{2\gamma}{1 + \gamma^2 \theta^2} \right)^2 \frac{A}{4\pi z^2} \tag{3.1}$$

$$E_\nu = \frac{0.43 E_\pi}{1 + \gamma^2 \theta^2}, \tag{3.2}$$

where E_π is the energy of the parent pion, m_π the mass of the parent pion, θ the angle between the pion and neutrino directions and $\gamma = E_\pi / m_\pi$.

Equations 3.1 and 3.2 and are shown as functions of neutrino energy and off-axis angle in Figure 3.2. Figure 3.3 shows the number of neutrino events as a function of the charged current ν_μ energy for the Low (left plot) and Medium (right plot) Energy Tune for various off-axis angles.

For the Medium Energy Tune, figure 3.2b shows that at 14 mrad the neutrino energy does not have a strong dependence on the parent pion energy. In addition, figure 3.3b shows that at 14 mrad the Medium Energy Tune produces a narrow energy neutrino beam with approximately 4 times more neutrinos at 2GeV than the on-axis scenario. This peak at 2 GeV is well matched to the expected energy of the oscillation maximum. The oscillation maximum for electron neutrino appearance in a muon neutrino beam is expected to occur at 1.6 GeV for NOvA's L/E and for $\Delta m^2_{32} = 2.4$ meV^2.

As described above, placing the detector off-axis increases the flux at the expected oscillation maximum. In addition the narrow energy range of the off-axis beam improves the rejection of background events. Neutral current events are an important background source whose topologies can be hard to distinguish from electron showers produced by ν_e CC events. For NC events the neutrino carries a significant amount of the energy away and the visible energy tends to "feed down" to lower energies. For narrow band off-axis beam this feed down tends to shift the neutral current events to lower energies outside the ν_e appearance signal energy window. Figure 3.4 shows the number of ν_μ, ν_e and NC events as a function of visible energy, the bulk of the NC events (black histogram) are shown to shift below the signal region (red-hatched histogram).

3.2 The NOvA Detectors

The NOvA experiment uses a near and far detector to measure neutrino oscillations. The near detector is used to measure the un-oscillated neutrino energy spectrum and the electron neutrino component of the beam. The un-oscillated neutrino energy spectrum measured by the near detector is extrapolated to the far detector (need to discuss further in a future chapter). The far detectors purpose is to measure the energy spectrum of the beam neutrinos for comparison with the extrapolated near detector energy spectrum.

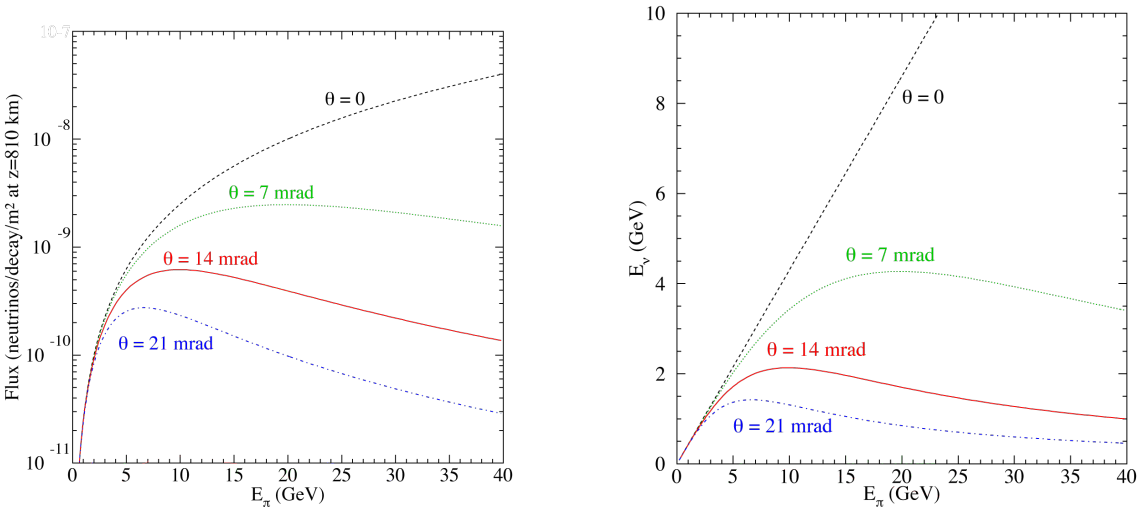

(a) Neutrino flux vs. pion energy.

(b) Neutrino energy vs. pion energy.

Figure 3.2: The above distributions are as viewed from a site located 800km from the NuMI target and off-axis by an angle θ.

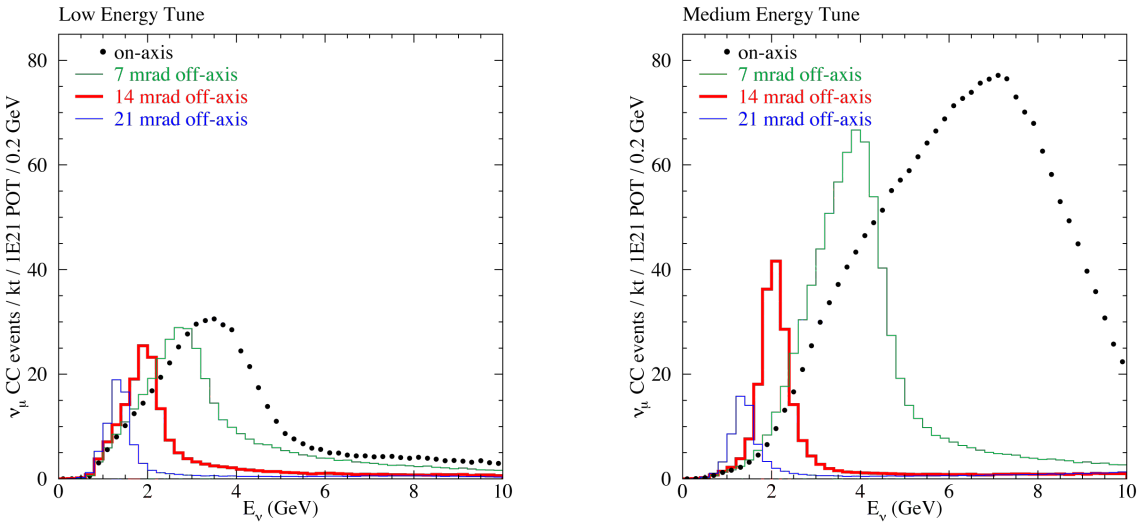

(a) Low Energy Tune neutrino energy.

(b) Medium Energy Tune neutrino energy.

Figure 3.3: Charged current ν_μ event rates vs. neutrino energy in the absence of oscillations. The distributions are found for a detector which is 800 km from the NuMI target and for various off-axis angles.

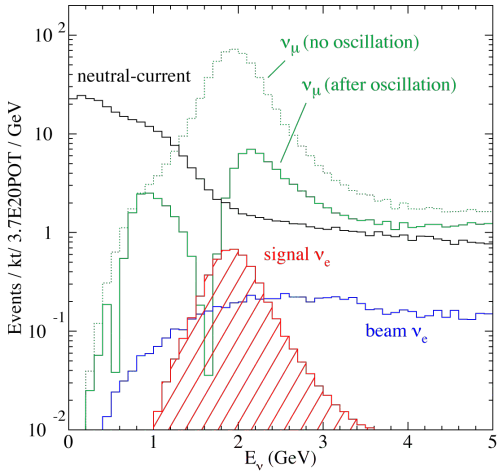

Figure 3.4: Simulated visible energy distributions for ν_μ CC events with and without oscillations, ν_e oscillation signal events, intrinsic beam ν_e events and neutral current events. The simulation assumes an off-axis position of 12 km at 810 km, $\Delta m^2 = 2.5 \times 10^{-3}\text{eV}^2$, $\sin^2(2\theta_{23}) = 1.0$ and $\sin^2(2\theta_{13}) = 0.1$.

The NOvA experiment aims to perform both $\nu\mu$ disappearance and nu_e appearance measurements. The detectors are designed to distinguish electron and muon neutrino charged current events from backgrounds.

The near and far NOvA detectors are almost functionally identical. Besides the different masses there are a few physical differences. The near detector has a so called "muon catcher", has a higher rate of readout and uses slightly different APDs. The construction common among both detectors will be discussed in the following section. The details specific to the far and near detectors will be discussed in Subsections 3.3.1 and 3.3.2 respectively.

3.2.1 The Basic NOvA Detector Element

The basic unit of both NOvA detectors is a rectangular rigid PVC cell which contains liquid scintillator and a wavelength-shifting (WLS) fibre. An illustration of the cell is shown in Figure 3.7. The WLS fibre, which is twice the length of the cell, is looped at the bottom of the cell such that the captured light travels in two directions to the instrument top end of the cell. At the top end of the cell each end of the looped fibre is directed onto one pixel of an Avalanche Photo Diode (APD) array. The APD converts the light from the fibre to a digital signal.

The NOvA cells are made from highly reflective titanium dioxide loaded rigid PVC. The cells have 2 and 4.5 mm thick walls, an interior depth of 5.9 cm along the beam

component	purpose	new mass fraction
mineral oil	solvent	94.63%
pseudocumene	scintillant	5.23%
PPO	waveshifter #1	0.140%
bis-MSB	waveshifter #2	0.0016%
Stadis-425	antistatic agent	0.0010%
tocopherol (Vit.E)	antioxidant	0.0010%
Total		100.00%

Figure 3.5: Liquid scintillator composition. Table taken from [3].

direction, an interior width of 3.8 cm transverse to the beam direction and an interior length of 15.5 m.

3.2.2 Liquid Scintillator

Approximately 70% of the NOvA detector mass is composed of the liquid scintillator within the cells. The composition of the liquid scintillator is shown in Figure 3.5. The scintillator is composed mainly of mineral oil along with 4.1% pseudocumene as the scintillant. The scintillant emits scintillation light with a spectrum peaked between 360 - 390 nm. Wavelength shifting chemical additives PPE and bis_MSB are added to shift the initial light spectrum to 400 - 450 nm to match the absorption spectra of the WLS fibre.

3.2.3 Wavelength Shifting Fibre

The WLS fibre has a diameter of 0.7 mm and a core of polystyrene mixed with 300 ppm R27 dye as the wave shifter. The fibre has two coatings of materials with a lower refractive index than the core which facilitates total internal reflection within the fibre. The fibre is first coated with a thin acrylic layer of PMMA and second with fluor-acrylic. These coatings make up about 3% of the fibre diameter.

The 400 - 450 nm light emitted by the scintillator is absorbed by the fibre and wavelength shifted to green light (490 - 550 nm). As light travels down the fibre it is attenuated, by a factor of about 10 in the FD, with red light (520 - 550 nm) preferentially surviving.

3.2.4 Avalanche Photo Diode

The light exiting the fibre ends is detected by an Avalanche Photodiode (APD), see Figure 3.6. An APD contains an array of 32 pixels, each pixel is interfaced with both ends of

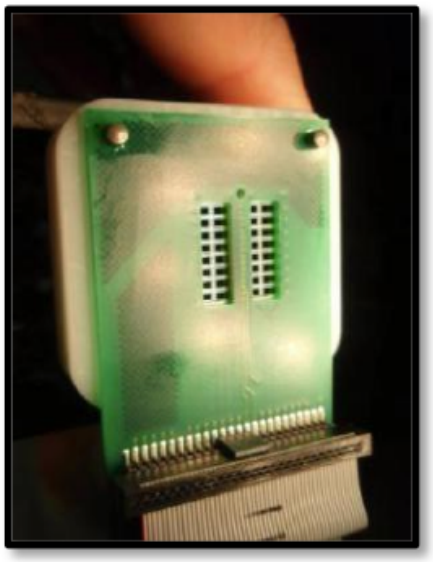

Figure 3.6: The NOvA APD containing an array of 32 pixels.

a single WLS fibre. The NOvA APD has an 85% quantum efficiency for the red light (520 - 550 nm) exiting the fibre ends. The thermal noise generated by each APD is reduced by thermo-electric coolers which cool the APDs to -15^{o}C. The excess heat is removed by a water cooling system.

3.2.5 Front End Board

A front end board (FEB) is connected to each APD. The signals from each APD are continously read out by the FEBs.

3.2.6 Detector Assembly

The NOvA detectors are constructed from the cells described in Section 3.2.1. 16 cells are extruded together in one unit to form an extrusion as shown in Figure 3.8.

Two extrusions are placed side by side to form an extrusion module consisting of 32 cells as shown in Figure 3.9. The module ends are capped by the end plate so that the modules can contain the liquid scintillator. The other end is capped by a manifold cover which contains the liquid scintillator in the horizontal cells and directs the 32 fibre end pairs to the 32 APD pixels in the NOvA APD.

Flat planes of cells are constructed from multiple modules glued together side by side. The planes layered with alternating orthogonal orientations, such that the orientation of the cells making up the plain alternate between horizontal and vertical from plane to plane (see Figure 3.10). The orthogonal orientation of the planes allows for three dimensional

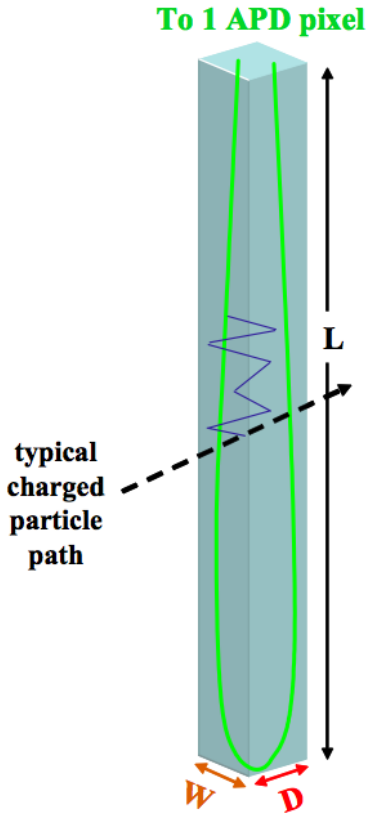

Figure 3.7: A NOvA cell consisting of an extruded PVC tube filled with liquid scintillator and a looped WLS fibre.

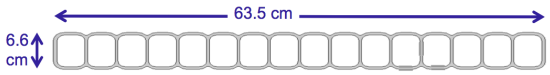

Figure 3.8: A side on view of an extrusion constructed from16 cells.

reconstruction of tracks passing through multiple planes. Planes are glued together in the orthogonal arrangement described above to form one solid detector piece called a block, consisting of 32 or 24 planes in the far detector or near detector respectively.

3.3 Data Acquisition System

NOvA's readout and data acquisition system (DAQ) are designed to concentrate data from all the channels into one stream to be analysed and stored. Data is stored in an intermediate location while online trigger processors analyse whether to record or reject the data.

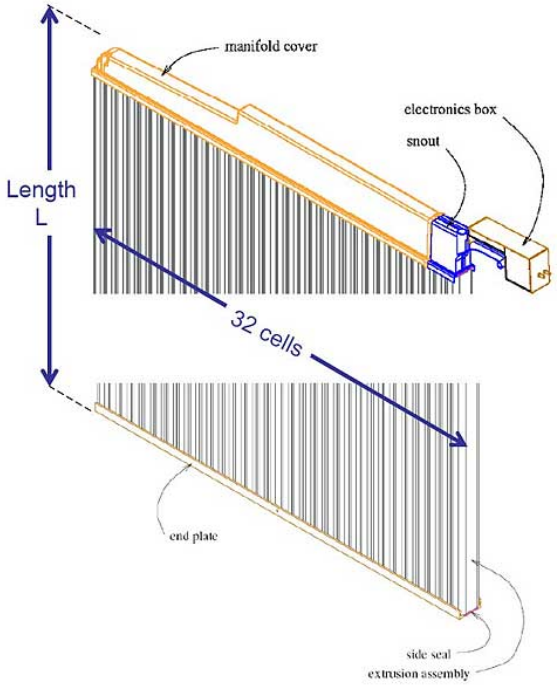

Figure 3.9: A side on view of an extrusion module constructed from two extrusions of 16 cells.

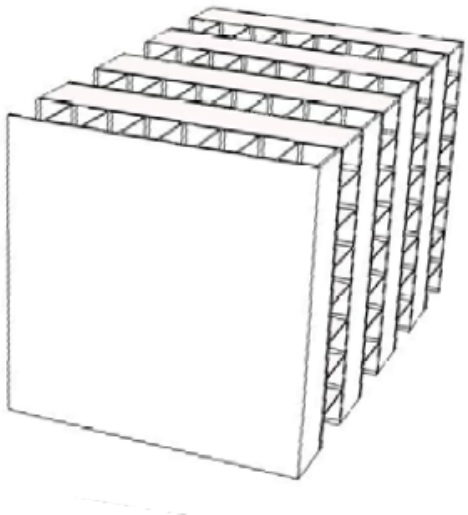

Figure 3.10: Cut out of a NOvA detector showing the alternating orientation of the stacked planes.

3.3.1 The Far Detector

The 14 kt far detector is located 810 km from the NuMI target, approximately 10 m below the surface and at an elevation of 372 m above sea-level. The neutrino beam enters the detector travelling at an angle of 3^o upwards. The detector is constructed, as described in Section 3.2.6, from 344,064 15.5 m long cells which form 896 planes normal to the beam direction. The detector mass is approximately 65% liquid scintillator and 35% PVC.

As described above, the far detector is built on the surface above sea level which means that cosmic rays will be a major source of background events. The background due to cosmic rays is mitigated using selection cuts and a shielding overburden above the detector. For the ν_μ disappearance analysis the background is primarily due cosmic ray muons which are removed using cuts. For the ν_e appearance analysis the background is primariy cosmic ray photons whose interactions within the detector can be mistaken for an electron shower.

During a six year run the FD without overburden shielding will see approximately 1600 background events due to cosmic ray photons. In order to reduce this background source to less than one event requires approximately 9 radiation lengths of material above the detector surface. Additional radiation lengths are desirable to contain any showers caused by interactions within the overburden. With this in mind the far detector building was constructed with a 122 cm thick concrete enclosure which supports a 15 cm thick overburden of barite. Together, the concrete enclosure and barite overburden provide 12 radiation lengths of shielding.

3.3.2 The Near Detector

The NOvA near detector is located on site at Fermilab next to the MINOS Hall as shown in Figure 3.11. The detector is 105 m underground and 1.015 km from the NuMI target. The detector therefore sees a higher flux of NuMI neutrino events and a lower flux of cosmic rays than the far detector. The neutrino beam enters the detector travelling downwards at an angle of 3^o downwards. A diagram of the near detector is shown in Figure 3.12. The detector is constructed in a similar fashion to the far detector from 20,192 cells arranged in 214 planes, each plane is comprised of 3 modules (except in the muon catcher). The detector has a width and height of 4.2 m and a length of 15.8 m. The near detector is functionally equivalent to the far detector with the exception of two distinguishing features.

First, a muon catcher is employed at the downstream end of the near detector. The muon catcher is constructed from layers of steel planes and planes of liquid scintillator cells.

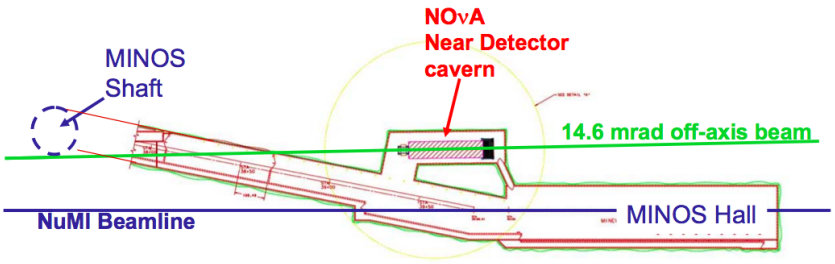

Figure 3.11: Bird's-eye view of NuMI Beamline, NOvA near detector cavern and the MINOS Hall.

The steel planes are 10 cm thick and are seperated by pairs of horizontal and vertically aligned planes of liquid scintillator cells. The vertical planes consist of three modules while the horizontal planes are made from just two modules. Therefore the sets of steel and scintillator planes are three modules wide (the same as the rest of the detector) but only two modules high. Ten of these steel and liquid scintillator plane sets are stacked to form the muon catcher. The downstream end of the muon catcher has an additional 3 liquid scintillator planes. The muon catcher is added to the downstream end of the near detector in order to help range out muons from few GeV charged current ν_μ interactions.

Second, the near detector electronics are setup to sample each channel four times more frequently (every 125 ns) than in the far detector to help handle the data pileup. The near detector sees approximately 5-10 neutrino interactions per beam spill (10 μs window) while the far detector sees approximately 60-70 cosmic rays per 550 μs window spread out over approximately 17 times more channels. The faster sampling rate improves the timing resolution of hits in the detector. With better timing resolution pileup events are more easily distinguished from one another.

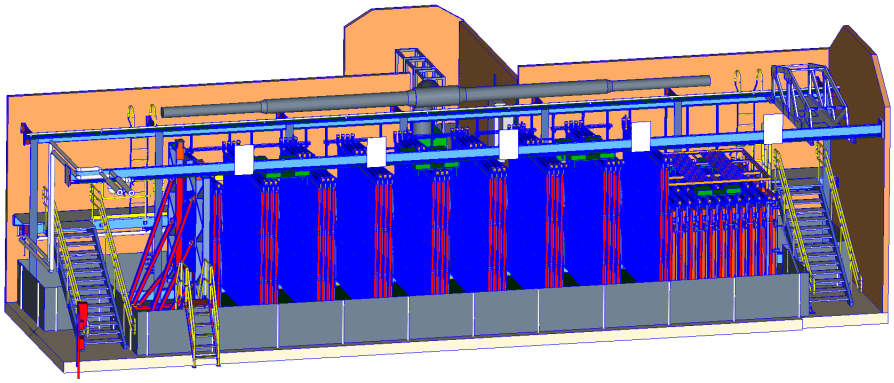

Figure 3.12: Technical drawing of the near detector and surrounding cavern. The NuMI beam enters from the left and the shorter muon catcher is shown on the right hand side of the detector. Note that only some of the planes have been drawn to aid visualisation.

Chapter 4

Energy Resolution

Energy resolution binning was implemented in MINOS to improve the sensitivity of the experiment. Techniques similar to those found in [2] will be used in the following chapter to improve the sensitivity of the NOvA experiment.

Bibliography

[1] D. S. Ayres et al. The NOvA Technical Design Report. *Fermilab Publication*, 2007. 4

[2] John Stuart Marshall. *A study of muon neutrino disappearance with the MINOS detectors and the NuMI neutrino beam.* PhD thesis, Cambridge U., 2008. 16

[3] Stuart L. Mufson. Scintillator update. *Internal NOvA document, DocDB-8541*, 2013. viii, 9